

Parameter sensitivity and its effect on agricultural productivity and drought occurrence in the Mahi River Basin

Anuj Kumar Dwivedi^{1,*}, Saral Kumar², Nisha Singh³, and Deepak Singh^{4,*}

¹Nation Institute of Hydrology Roorkee-247667, Uttarakhand, India

²Sam Higginbottom University of Agriculture, Technology and Sciences, Prayagraj-211007, Uttar Pradesh, India

³University of Lucknow, Lucknow, 226007, India

⁴ICAR-Indian Institute of Soil & Water Conservation, RC-Datia, 475661, India

*Corresponding author email: akdwivedi2009@gmail.com; dpk905@gmail.com

Received : June 21, 2025
Revised : August 22, 2025
Accepted : August 23, 2025
Published : December 31, 2025

ABSTRACT

Present study provides an in-depth analysis of climate variables, drought indices, and agricultural productivity from 1985 to 2022, uncovering significant trends in regional climatic and agricultural dynamics. Maximum temperatures consistently ranged from 40°C to 50°C, while the average temperature increased by approximately 1.2°C, reflecting the impacts of global warming on evapotranspiration and agricultural systems. Annual precipitation exhibited notable variability, with dry years (e.g., 1987, 1992, and 2002) receiving less than 300 mm, and wet years (e.g., 1995, 2007, and 2021) receiving over 700 mm. Despite these fluctuations, no clear long-term trend in precipitation was observed. Drought indices, such as SPI, RAI, and SAI, revealed significant drought events in the late 1980s, early 1990s, and mid-2000s, with wetter years observed in 1994, 2006, and 2019. Relative humidity remained fairly stable, averaging around 65%, but its relationship with drought indices highlighted the role of reduced atmospheric moisture in intensifying drought severity. The analysis of drought indices and yield anomalies indicated mixed correlations. Severe droughts were associated with negative SPI, RAI, and SAI values, while improved hydrological conditions were evident in recent years (2020–2022). Statistical analysis showed that the Yield Anomaly Index (YAI) had a minimal correlation with SPI ($R^2 = 0.0031$), suggesting that precipitation alone has little impact on yield anomalies. However, moderate correlations were found between YAI and SAI ($R^2 = 0.245$) and YAI and RAI ($R^2 = 0.1487$), implying that rainfall anomalies and climate conditions partially influence yield variability. The low R^2 values indicate that other factors, such as temperature, soil conditions, and agricultural practices, play a significant role in yield performance. These findings underscore the need to integrate multiple climatic and agronomic factors into water and agricultural management strategies to enhance climate resilience and ensure sustainable development in the region.

Keywords: Climate variables, Drought indices, Agricultural productivity, Yield Anomaly Index (YAI), Precipitation variability

INTRODUCTION

Accurately measuring drought, a complex natural phenomenon, can be challenging (Quiring, 2010). While drought is most prevalent in arid regions, it can occur worldwide, even in areas with high humidity and rainfall (Dai, 2011). The American Meteorological Society categorizes

drought into four types: meteorological, agricultural, hydrological, and social and economic (Heim, 2002). This study concentrates on agricultural drought, which is characterized by insufficient soil moisture over a specific period, resulting in crop failure (Mishra and Singh, 2010). Agricultural drought can impact various stages of crop growth, leading to

diverse reductions in crop yield. The assessment of agricultural drought and its impact on crop production is further complicated by the significant spatial and temporal variations in drought frequency, timing, and intensity. Researchers have created drought indices as effective tools for identifying, tracking, and assessing drought events (Niemeyer, 2008). In recent decades, over 150 such indices have been developed for various locations, purposes, and applications (Zargar *et al.*, 2011). Initially, conventional meteorological measurements like rainfall and temperature were utilized to construct these indices (Wu *et al.*, 2013), including the Standardized Precipitation Index (SPI; McKee *et al.*, 1993), the Palmer drought severity index (PDSI; Palmer, 1965), and the moisture anomaly index (Z-index; Palmer, 1965). While these meteorological drought indices typically performed well at individual weather stations, their effectiveness diminished at a regional scale due to insufficient station coverage across large areas. Consequently, the sparse meteorological data often available over extensive regions is generally inadequate to support prompt drought detection, monitoring, and decision-making processes (Son *et al.*, 2012; Unganai and Kogan, 1998).

Remote sensing data provides a valuable alternative to station-based data, as it enables drought monitoring on a large scale, particularly in regions with low population density and harsh environmental conditions (Rhee *et al.*, 2010; Wu *et al.*, 2013; Mandal *et al.*, 2025). For more than three decades, various remotely sensed drought indices have been developed for drought monitoring (Peng *et al.*, 2015). Table 1 presents several widely utilized remotely sensed drought indices. Although drought indices continue to evolve and improve, accurately assessing drought remains a complex task, and the universal applicability of remote sensing indices is not well-established. Evaluating various drought indices side by side can enhance our understanding

of drought events and provide a comprehensive analysis of their effectiveness (Zhang *et al.*, 2017). Research by Morid, Smakhtin, and Moghaddasi (2006) indicated that employing multiple indices is necessary for more precise results, given the varying responses of different indices to local conditions. Bayarjargal *et al.*, (2006) noted the difficulty in identifying the most reliable drought index and found that the accuracy of local meteorological measurements was insufficient to validate remotely sensed drought indices across extensive areas. A study conducted by Zhang *et al.*, (2017) examined the utility of 13 remotely sensed drought indices across the Continental United States for drought analysis, revealing that the performance of these indices varied across climate zones. They suggested that future development of combined indices should focus more on empirical weighting based on climate factors. Consequently, proposing a single drought index capable of accurately monitoring drought conditions throughout a large region proves challenging due to the complexity of landscapes and climates.

Agricultural drought primarily manifests as a decrease in crop production. Research by Quiring and Papakryiakou (2003) revealed a statistically significant correlation between the Z-index and Red Spring wheat yield across all crop districts, though the strength of these correlations varied. In China, Wang *et al.*, (2016) compared soil moisture measurements with five climate-based drought indices to assess drought threats to winter wheat. Similarly, Tian, Yuan, and Quiring (2018) evaluated six drought indices for monitoring agricultural drought in the south-central United States. Both studies concluded that SPEI outperformed other indices, attributing this to SPEI's ability to define wet and dry periods using the balance between precipitation and potential evapotranspiration. Zhang, Mu, and Huang (2016) discovered that DSI effectively monitored agricultural drought severity at the provincial level in northern China. Anderson *et al.*, (2016) conducted drought monitoring in eight major agricultural states in eastern Brazil using ESI, finding it superior in predicting drought impacts on the yields of key crops such as soybean, maize, and wheat.

Agricultural drought varies in occurrence and intensity across space and time, and remote sensing drought indices have diverse applications. Consequently, it is essential to compare these indices

Table 1. SPI value classification

SPI Value	Class
2.0≥	Extremely Wet
1.5 to 1.99	Very Wet
1.0 to 1.49	Moderately Wet
0.99 to -0.99	Near Normal
-1 to -1.49	Moderately Dry
-1.50 to -1.99	Severely Dry
Below -2.0	Extremely Dry

to understand the drought event process and examine its effects on winter wheat yield over large areas. This research assessed the effectiveness of three commonly employed remote sensing drought indices (VHI, DSI, and TVDI) for monitoring agricultural drought in Shaanxi and Henan provinces within the North China Plain. The study focused on the primary winter wheat growing season from 2000 to 2013. To evaluate and contrast the agricultural drought monitoring capabilities of these remote sensing indices, we utilized SPI, winter wheat yield data, soil moisture measurements, and NMDM maps.

MATERIALS AND METHODS

Study Area

The Mahi River Basin encompasses the states of Madhya Pradesh, Rajasthan, and Gujarat, encompassing a total area of 34,842 square kilometers, with a maximum length of approximately 330 km and a width of approximately 250 km. It is situated between longitudes 72°21' and

75°19' east and latitudes 21°46' and 24°30' north. The basin is delineated by the Aravalli Hills to the north and northwest, the Malwa Plateau to the east, the Vindhya Range to the south, and the Gulf of Khambhat to the west. The Mahi River, one of India's significant west-flowing interstate rivers, originates from the northern slopes of the Vindhyas at an elevation of 500 m, near the village of Bhopawar in the Sardarpur tehsil of Dhar district, Madhya Pradesh. The river extends 583 km, with the Som River as its primary tributary joining from the right, and the Anas and Panam Rivers entering from the left, ultimately discharging into the Arabian Sea through the Gulf of Khambhat. Agricultural land constitutes 63.63% of the basin, while water bodies account for 4.34%. The basin encompasses 11 parliamentary constituencies (as of 2009), with 6 in Gujarat, 3 in Rajasthan, and 2 in Madhya Pradesh. Fig. 1 illustrates the study area, highlighting the Mahi Basin and its network of hydrological observation stations. These stations serve a crucial function in monitoring various hydrological parameters, including river flow and precipitation.

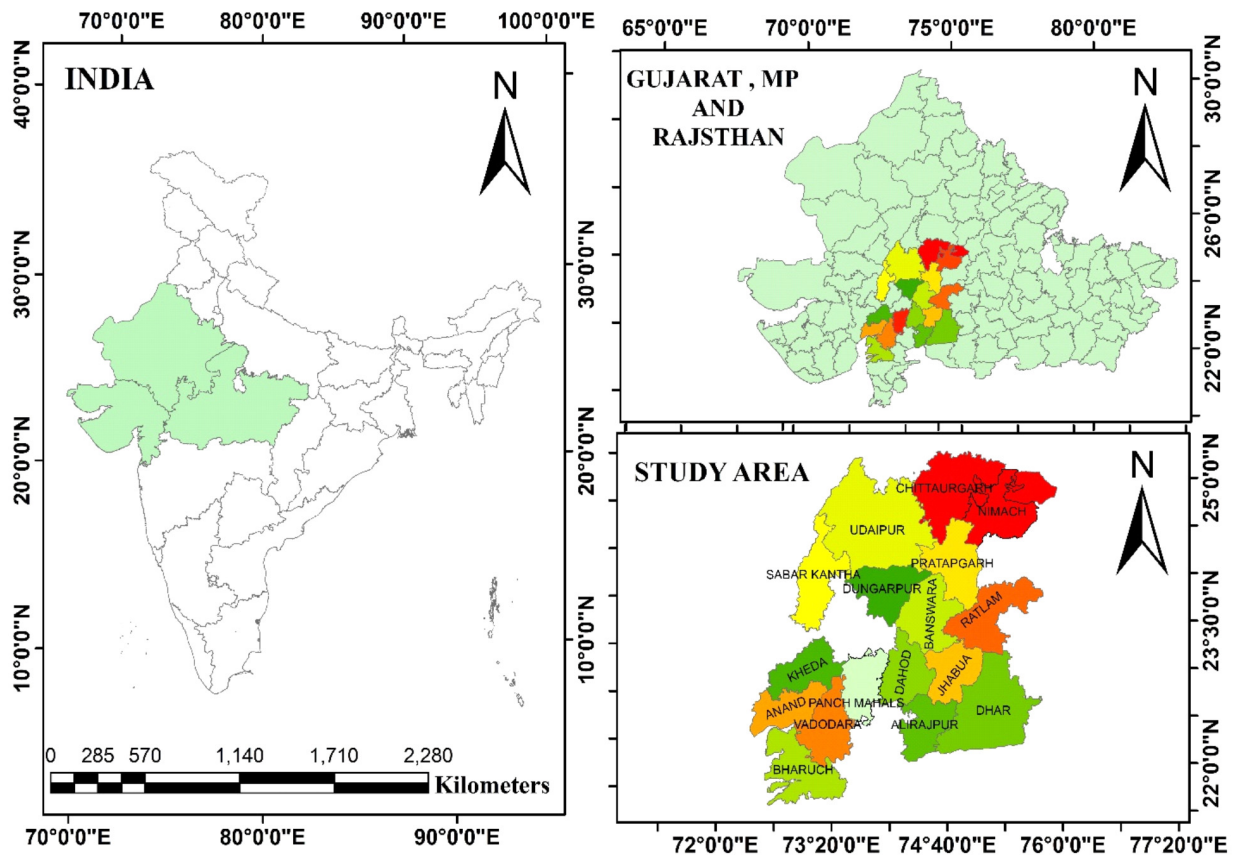


Fig. 1. Study Area (Mahi Basin with hydrological observation stations)

The spatial distribution of these observation points is essential for comprehending the basin's hydrological dynamics, facilitating effective water resource management, flood control, and environmental monitoring in the region.

Standardized Precipitation Index (SPI)

SPI was developed by Mckee et al., (1993) and is based just on precipitation and therefore requires less input data and calculation efforts. Along term precipitation record at the desired station is fitted to a probability distribution (e.g. Gamma Distribution), which is then transformed in to normal distribution so that the mean SPI is zero (Edwards and Mckee, 1997). SPI may be computed with different time steps (e.g. 1 month, 3 months, 48 months) and is reported to be able of identify emerging droughts sooner than the Palmer Index. The use of different time scales under the umbrella of the same index allows the effects of precipitation deficit on different water resources components (ground water, reservoir storage, soil moisture, stream flow) to be assessed.

SPI is one of the most versatile and popular droughts indices which is used for meteorological droughts characterization and classification. Gama distribution probability density function is used to calculate the SPI. It is represented by g(x) and by the given below formula:

$$g(x) = \frac{1}{\beta^\alpha \Gamma(\alpha)} x^{\alpha-1} \cdot e^{-\frac{x}{\beta}}, x > 0 \quad \dots(1)$$

Where $\Gamma(\alpha)$ is the gamma function; x (mm) is the amount of precipitation ($x>0$); α is the shape parameter ($\alpha>0$); and β is the scale parameter ($\beta>0$). SPI and RDI value classification is given in Table 1.

Standardised Anomaly Index (SAI)

Introduced by Kraus in the mid-1970s and was examined closely by Katz and Glantz at the National Center for Atmospheric Research, United States, in the early 1980s. SAI was developed based on RAI, and RAI is a component of SAI. They are similar, but both are unique are as shown as in Table 2.

$$SAI = \frac{X-\mu}{\sigma} \quad \dots(2)$$

Where,

X=Current Month/Year/Seasonal Rainfall Total(mm)

μ =Mean Annual Rainfall over a period of observation

Table 2. Categorization of SAI values

SAI Value	Category
Above 2	Extremely Wet
1.5 to 1.99	Very Wet
1.0 to 1.49	Moderately Wet
-0.99 to 0.99	Near Normal
-1.0 to -1.49	Moderately Dry
-1.5 to -1.99	Severely Dry
-2 or less	Extremely Dry

σ =Standard Deviation of Annual Rainfall over the period of observation

Rainfall Anomaly Index (RAI)

It was introduced by Van-Rooy in 1965 and is based on calculated precipitation against random values from -3 to +3; as the irregularities of precipitation assigned 10 bounds. The only effective factor in this index is precipitation. It is applied in both monthly and annual time scale as well.

The steps to calculate rainfall anomaly index (RAI) is as follow:

1. Calculate the long term average of monthly precipitation (P) in given station.
2. Extract the mean of 10 values of the maximum precipitation occurred in statistical period (m).
3. Extract the mean of 10 values of the minimum precipitation occurred in statistical period (X).
4. Compare the monthly precipitation data (P) to long term mean.

$$RAI = 3 \left[\frac{P-\bar{P}}{m-\bar{P}} \right] \quad \dots(3)$$

And if P is less than \bar{P} then RAI is given by

$$RAI = -3 \left[\frac{P-\bar{P}}{\bar{X}-\bar{P}} \right] \quad \dots(4)$$

In the former the abnormality is positive and in the latter is negative.

5. Assign +3 and -3 thresholds to the means of 10 maximum positive abnormalities and 10 minimums negative abnormalities, respectively. Table 3 presents classification of drought severity in terms of rainfall anomaly index.

Table 3. Classification of drought severity by RAI

Category	RAI value
Normal	0 to 3
Weak Drought	-1/0 to 0/3
Moderate Drought	-1/5 to -1/2
Severe Drought	-3 to -1/5
Extreme Drought	Less than -3

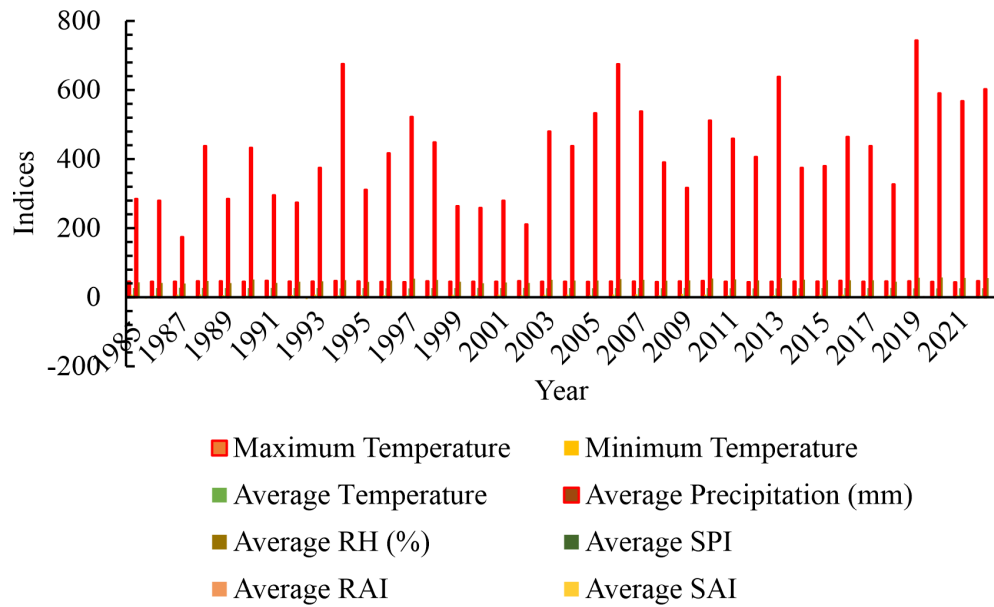


Fig. 2. Trends in Climate Variables and Drought Indices (1985–2022)

Fig. 2 illustrates the trends in climate variables and drought indices from 1985 to 2022, encompassing parameters such as maximum and minimum temperatures, average temperature, average precipitation, relative humidity (RH), and drought indices (RAI, SPI, and SAI). A consistent increase in maximum and average temperatures is observed over the years, indicative of rising global warming impacts. The precipitation trend demonstrates significant inter-annual variability, with notable peaks and troughs, suggesting sporadic rainfall events contributing to fluctuating drought conditions. The drought indices (RAI, SPI, and SAI) highlight periods of drought severity, with a general upward trend reflecting increased aridity in recent

decades. The interplay between temperature, humidity, and precipitation trends emphasizes the complex nature of climate systems and the potential implications for water availability and agricultural sustainability in the studied region.

The annual variations in the mean Standardized Precipitation Index (SPI), Rainfall Anomaly Index (RAI), and Standardized Anomaly Index (SAI) from 1985 to 2022 is illustrated in Fig. 3. These indices collectively elucidate the magnitude and frequency of drought conditions over the observed period. Significant negative values, particularly evident during the late 1980s, early 1990s, and mid-2000s, indicate periods of severe drought, with SPI and SAI demonstrating strong correlation in signifying

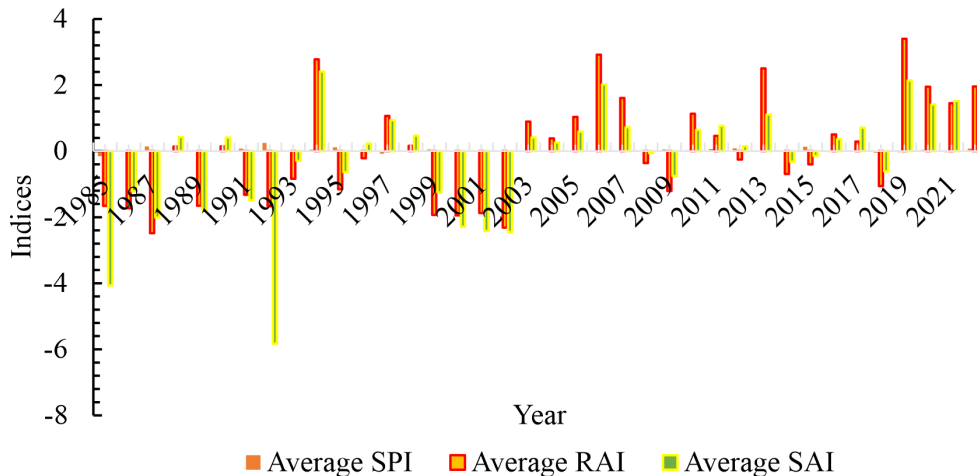


Fig. 3. Annual Variations in Average SPI, RAI, and SAI Indices (1985–2022)

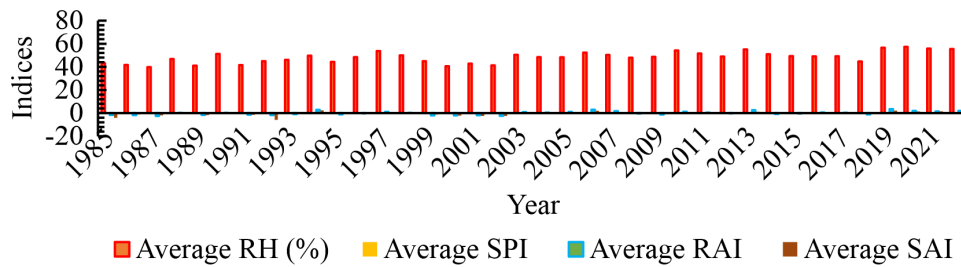


Fig. 4. Comparison of Average Relative Humidity (%) and Drought Indices (SPI, RAI, SAI) Over the Years (1985–2022)

precipitation deficits and broader climatic anomalies. Conversely, maxima in the positive range, notably during the late 1990s and circa 2010, suggest periods of excessive rainfall or improved moisture conditions. The persistent fluctuations indicate a dynamic climate system characterized by recurrent drought episodes, interspersed with periods of increased precipitation. These variations underscore the significance of monitoring these indices to anticipate and mitigate drought impacts on agriculture, water resources, and ecosystems. The temporal trend suggests increasing variability, potentially attributable to evolving climatic patterns.

The comparison of average relative humidity (RH%) and drought indices (SPI, RAI, and SAI) from 1985 to 2022 is illustrated in Fig. 4. Relative humidity remains relatively stable over the years, indicating limited direct influence of short-term climate variability. In contrast, the drought indices exhibit substantial interannual fluctuations, with notable decreases representing drought episodes and increases indicating wetter conditions. The alignment of negative indices with lower humidity levels demonstrates the correlation between reduced

atmospheric moisture and drought severity. While relative humidity appears more consistent, the variability in SPI, RAI, and SAI underscores the complex interplay of precipitation patterns, temperature, and atmospheric dynamics in shaping drought conditions. These findings emphasize the necessity to consider multiple indices and climatic parameters for effective drought monitoring and mitigation strategies.

The annual precipitation levels, measured in millimeters (mm), over a 36-year period is illustrated in Fig. 5. The bar graph demonstrates significant interannual variability, indicating fluctuating climatic patterns. The highest precipitation appears to have occurred in years such as 1995, 2007, and 2021, exceeding 700 mm. Conversely, the years with notably low precipitation, such as 1987, 1992, and 2002, recorded less than 300 mm. A discernible pattern of alternating dry and wet years suggests potential cyclical weather patterns or the influence of external climatic phenomena such as El Niño and La Niña. Despite the variability, no clear upward or downward trend is evident, indicating a relatively stable average annual precipitation across the studied

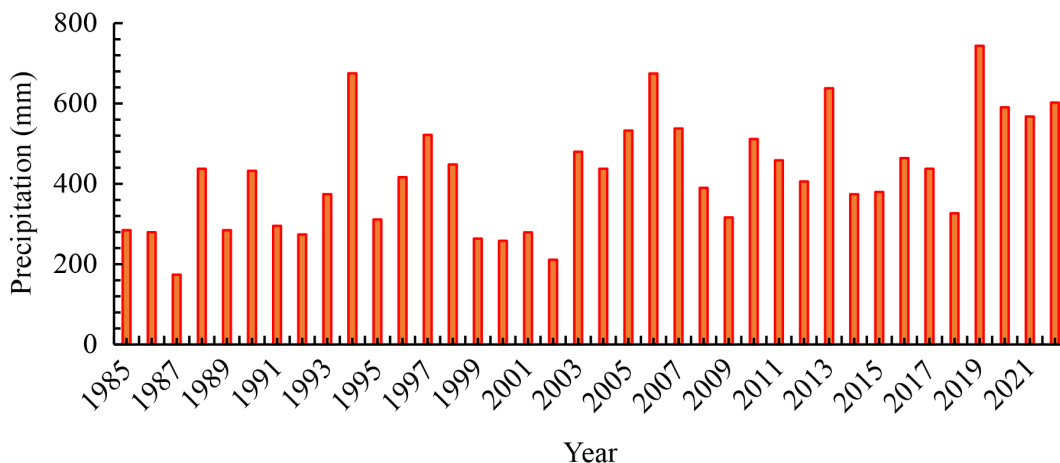


Fig. 5. Annual Precipitation Trends (1985-2021)

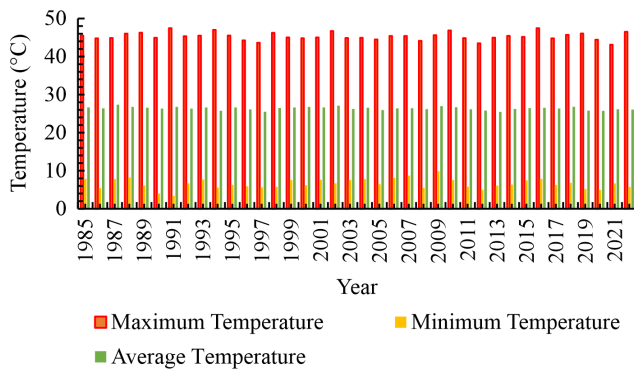


Fig. 6. Annual Temperature Variations (1985-2021)

period. This analysis provides valuable insight for understanding long-term climatic trends and planning for water resource management.

The trends in maximum, minimum, and average temperatures over a 36-year period is illustrated in Fig. 6. The red bars represent the maximum temperatures, consistently ranging between 40–50°C, indicating high annual peaks. The yellow bars denote minimum temperatures, which generally range between 0°C and 20°C, exhibiting considerable variation across the years. The green bars depict average temperatures, which remain relatively stable, fluctuating between 15°C and 30°C. The consistent range of maximum and minimum temperatures suggests a stable thermal amplitude over the years, with no substantial long-term increase or decrease observed. These data highlight the persistence of extreme heat events, which may pose challenges for agriculture, water resource management, and public health. The notable difference between maximum and minimum temperatures emphasizes significant diurnal and seasonal variability, which is critical for understanding local climate dynamics and implementing climate adaptation strategies.

The summary is presented in Table 4, depicting average drought indices (SPI, RAI, SAI) from 1985 to 2022, demonstrates a complex pattern of drought conditions throughout the study period. Years exhibiting significantly negative SPI, RAI, and SAI values, such as 1985, 1992, and 2002, indicate severe drought events. Conversely, periods characterized by positive values across indices, such as 1994, 2006, and 2019, reflect increased precipitation or recovery from drought conditions. It is noteworthy that RAI frequently exhibits more pronounced fluctuations compared to SPI and SAI, underscoring its sensitivity to extreme precipitation anomalies. The elevated positive indices observed in recent years,

Table 4. Summary of Average Drought Indices (SPI, RAI, SAI) by Year (1985–2022)

Year	Average SPI	Average RAI	Average SAI
1985	-0.15430335	-1.65635213	-4.063449968
1986	-2.48167E-16	-1.726502972	-1.215564583
1987	0.14253104	-2.483162522	-2.008678592
1988	5.48581E-16	0.137890255	0.429346476
1989	-0.000158123	-1.654913313	-1.775568573
1990	-6.26949E-16	0.142876162	0.409310878
1991	0.076902343	-1.323040218	-1.483325074
1992	0.25	-1.665366411	-5.829222011
1993	0	-0.834306412	-0.294269595
1994	0.045661125	2.776192915	2.409209196
1995	0.117608902	-1.152722967	-0.638628984
1996	5.61642E-16	-0.213860034	0.226585586
1997	-0.078903338	1.066733901	0.935920736
1998	-1.09716E-15	0.16021317	0.470965593
1999	0.049525008	-1.932854888	-1.250881653
2000	4.44089E-16	-1.945172877	-2.287259632
2001	-9.63282E-16	-1.873091143	-2.416374121
2002	7.05318E-16	-2.314948797	-2.450669785
2003	0.026159605	0.893151593	0.410576976
2004	0	0.387660113	0.257587306
2005	0.0228039	1.033836439	0.586886719
2006	-3.13475E-16	2.920784041	2.018733315
2007	5.11038E-05	1.609800886	0.719950266
2008	2.15514E-16	-0.36009044	-0.057676381
2009	0.049249225	-1.20592442	-0.752662725
2010	0.029499438	1.131598665	0.641094989
2011	0.065324337	0.458827712	0.766042512
2012	0.084554289	-0.252591748	0.146208458
2013	0.024220185	2.505356832	1.105779908
2014	-1.05798E-15	-0.692814961	-0.321293975
2015	0.134955995	-0.398513888	-0.147666769
2016	-0.028746146	0.504694369	0.366008799
2017	-1.67187E-15	0.287199533	0.707046095
2018	-0.046157216	-1.057543445	-0.613531876
2019	-0.032518269	3.400499679	2.138616107
2020	0.038352677	1.949660453	1.408351036
2021	-0.031608354	1.451167832	1.514981318
2022	0.078812384	1.958170235	2.12421095

particularly from 2020 to 2022, suggest improved hydrological conditions, potentially influenced by climatic variability or regional interventions. The observed trends emphasize the necessity for continuous monitoring and adaptive water resource management strategies to address the variability in drought conditions.

The relationship between the Average Yield Anomaly Index (YAI) and the Average Standard Precipitation Index (SPI) is illustrated in Fig. 7. The fitted linear regression equation is $y = 0.0474x + 0.0183$, with an exceptionally low coefficient of determination ($R^2 = 0.0031$), indicating that merely 0.31% of the variation in SPI is explained

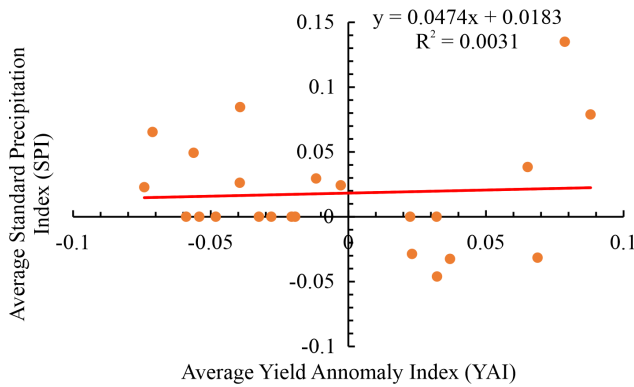


Fig. 7. Relationship Between Average Yield Anomaly Index (YAI) and Average Standard Precipitation Index (SPI)

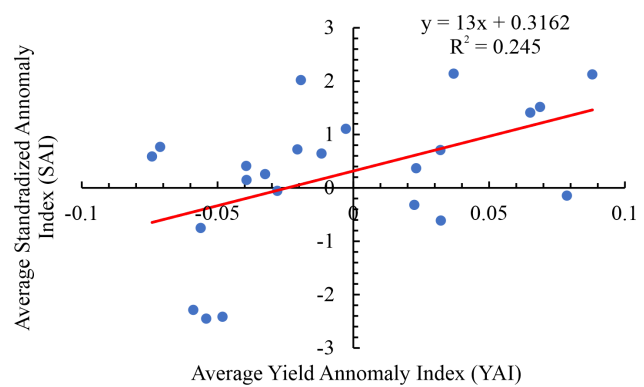


Fig. 8. Relationship Between Average Yield Anomaly Index (YAI) and Average Standardized Anomaly Index (SAI)

by YAI. The negligible slope of the regression line and the substantial dispersion of data points corroborate the absence of a significant linear relationship between these variables. This lack of correlation suggests that SPI, as an indicator of precipitation, exerts minimal influence on yield anomalies in this context. Alternative factors such as temperature, soil conditions, or management practices may exert a more substantial impact on YAI. Subsequent analysis incorporating additional variables and advanced statistical methodologies could elucidate stronger predictors of yield anomalies and potential non-linear relationships within the dataset.

The relationship between the Average Yield Anomaly Index (YAI) and the Average Standardized Anomaly Index (SAI) is illustrated in Fig. 8. The regression equation $y = 13x + 0.3162$ and the coefficient of determination ($R^2 = 0.245$) indicate a moderate positive correlation, wherein 24.5% of the variation in SAI is explained by YAI. The positive slope of the regression line suggests that higher YAI values are generally associated with higher SAI values. However, the majority of the variability in SAI remains unexplained, implying that additional environmental or external factors likely influence SAI. Further research incorporating additional variables and advanced modeling techniques could potentially elucidate the factors driving this relationship more comprehensively.

The relationship between the Average Yield Anomaly Index (YAI) and the Average Rainfall Anomaly Index (RAI) is illustrated in Fig. 9. The linear regression equation, $y = 12.054x + 0.5086$, and the

coefficient of determination, $R^2 = 0.1487$, indicate a weak positive correlation.

This result suggests that variations in rainfall anomalies exert a moderate influence on yield anomalies; however, the low R^2 value (14.87%) implies that additional factors contribute significantly to yield variability. The dispersed data points highlight inconsistent relationships, necessitating further investigation into supplementary variables such as soil quality, crop type, and agricultural practices to achieve a more comprehensive understanding.

A comparative analysis of the actual yield (T/Ha) and the Yield Anomaly Index (YAI) across various observations demonstrate congruent trends, with yield fluctuations closely corresponding to variations in the YAI (Fig. 10). This correlation suggests that the YAI effectively captures yield variability. Significant peaks and troughs in the data likely correspond to specific environmental or management factors influencing crop production.

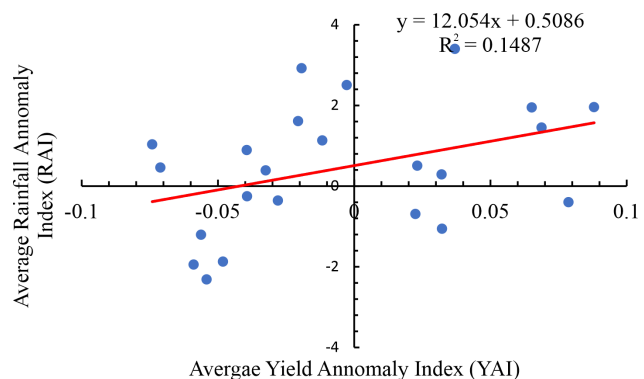


Fig. 9. Relationship Between Average Rainfall Anomaly Index (RAI) and Average Yield Anomaly Index (YAI)

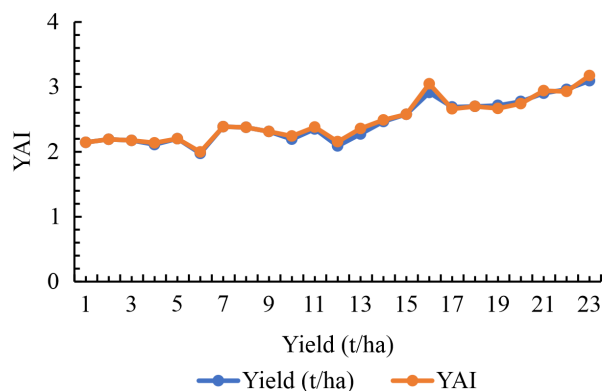


Fig. 10. Comparison of Yield (t/ha) and Yield Anomaly Index (YAI)

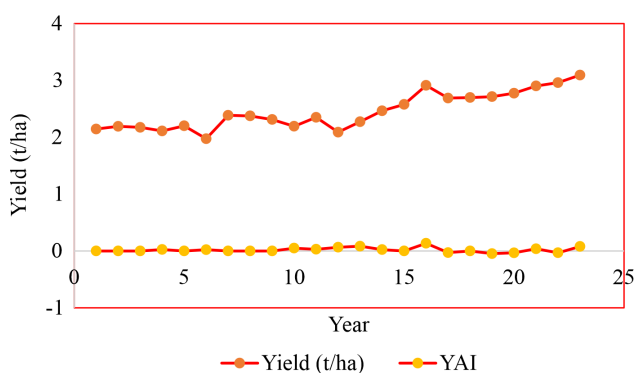


Fig. 11. Temporal Trends in Yield (t/ha) and Yield Anomaly Index (YAI)

The observed consistency between yield and YAI trends indicates that YAI serves as a reliable indicator for assessing yield performance relative to expected values, thus rendering it a valuable tool for agricultural monitoring and planning.

Yield (t/ha) exhibited a gradual upward trajectory with periodic fluctuations, indicating an overall enhancement in agricultural productivity (Fig. 11). Conversely, YAI remains relatively constant around zero, suggesting that yield anomalies are minimal and predominantly consistent with expected values over the years. The correlation between both trends implies that yield variability is adequately accounted for by the anomaly index, rendering it a reliable metric for monitoring year-to-year variations in crop performance.

CONCLUSION

The analysis of climate variables, drought indices, and yield anomalies from 1985 to 2022 reveals significant climatic variability and its implications for drought dynamics and agricultural

productivity in the study region. Maximum temperatures consistently ranged between 40–50 °C, with mean temperatures increasing by about 1.2 °C over the study period, indicating the influence of global warming and its potential effects on evapotranspiration and crop stress. Annual rainfall showed strong inter-annual variability, ranging from below 300 mm in drought years (e.g., 1987, 1992, and 2002) to over 700 mm in wet years (e.g., 1995, 2007, and 2021), though no clear long-term trend was evident. Drought indices (SPI, RAI, and SAI) identified recurrent severe drought episodes during the late 1980s, early 1990s, and mid-2000s, interspersed with wetter phases in the late 1990s and around 2010. Relative humidity remained relatively stable at approximately 65%, yet its association with drought indices suggests that reduced atmospheric moisture, combined with rainfall deficits, intensified drought severity. Recent improvements in drought conditions during 2020–2022 reflect both climatic variability and possible effects of regional water management interventions. Correlation analysis between drought indices and yield anomaly index (YAI) shows weak to moderate relationships. SPI exhibited negligible influence on yield variability ($R^2 = 0.0031$), whereas SAI ($R^2 = 0.245$) and RAI ($R^2 = 0.1487$) showed moderate positive associations, highlighting the role of rainfall anomalies and standardized conditions. However, the low explanatory power of these indices indicates that crop yields are also strongly influenced by temperature extremes, soil properties, and agricultural management practices.

ACKNOWLEDGEMENT

The author thanks to the dean Vaugh Institute of Engineering & Technology, SHUATS-Allahabad for providing necessary facility to conduct the research work.

DATA AVAILABILITY STATEMENT

All relevant data used in present study may be obtain on reasonable request of corresponding author.

CONFLICT OF INTEREST

The authors declare there is no conflict.

REFERENCES

Anderson, M.C., Zolin, C.A., Sentelhas, P.C., Hain, C.R., Semmens, K., Yilmaz, M.T., and Tetrault, R. (2016).

- The Evaporative Stress Index as an indicator of agricultural drought in Brazil: An assessment based on crop yield impacts. *Remote Sensing of Environment*, 174, 82-99.
- Bayarjargal, Y., Karnieli, A., Bayasgalan, M., Khudulmur, S., Gandush, C., and Tucker, C.J. (2006). A comparative study of NOAA–AVHRR derived drought indices using change vector analysis. *Remote Sensing of Environment*, 105(1), 9-22.
- Dai, A. (2011). Drought under global warming: a review. *Wiley Interdisciplinary Reviews: Climate Change*, 2(1), 45-65.
- Edwards, D.C., and McKee, T.B. (1997). Characteristics of 20th century drought in the United States at multiple time scales.
- Heim Jr, R.R. (2002). A review of twentieth-century drought indices used in the United States. *Bulletin of the American Meteorological Society*, 83(8), 1149-1166.
- Mandal, U.K., Ghosh, A., Karim, F., Mallick, S., Nayak, D.B., Bhutia, R.N., Bhardwaj, A.K., Lama, T.D., Burman, D., Choudhury, P., Mahanta, K.K., Raut, S., Mandal, S., Mainuddin, M. (2025) Land use change and soil salinization in the Sundarbans: a machine-learning based analysis of long-term transformation and future projections. *Environ Monit Assess* 197, 1380. <https://doi.org/10.1007/s10661-025-14829-2>
- McKee, T.B., Doesken, N.J., and Kleist, J. (1993, January). The relationship of drought frequency and duration to time scales. In *Proceedings of the 8th Conference on Applied Climatology* (Vol. 17, No. 22, pp. 179-183).
- Mishra, A.K., and Singh, V.P. (2010). A review of drought concepts. *Journal of hydrology*, 391(1-2), 202-216.
- Morid, S., Smakhtin, V., and Moghaddasi, M. (2006). Comparison of seven meteorological indices for drought monitoring in Iran. *International journal of climatology*, 26(7), 971-985.
- Niemeyer, S. (2008). New drought indices. *Options Méditerranéennes. Série A: Séminaires Méditerranéens*, 80, 267-274.
- Palmer, W.C. (1965). *Meteorological drought* (Vol. 30). US Department of Commerce, Weather Bureau.
- Peng, C., Deng, M., and Di, L. (2014). Relationships between remote-sensing-based agricultural drought indicators and root zone soil moisture: a comparative study of Iowa. *IEEE Journal of Selected Topics in Applied Earth Observations and Remote Sensing*, 7(11), 4572-4580.
- Quiring, S.M., and Ganesh, S. (2010). Evaluating the utility of the Vegetation Condition Index (VCI) for monitoring meteorological drought in Texas. *Agricultural and Forest Meteorology*, 150(3), 330-339.
- Quiring, S.M., and Papakryiakou, T.N. (2003). An evaluation of agricultural drought indices for the Canadian prairies. *Agricultural and Forest Meteorology*, 118(1-2), 49-62.
- Rhee, J., Im, J., and Carbone, G.J. (2010). Monitoring agricultural drought for arid and humid regions using multi-sensor remote sensing data. *Remote Sensing of Environment*, 114(12), 2875-2887.
- Son, N.T., Chen, C.F., Chen, C.R., Chang, L.Y., and Minh, V.Q. (2012). Monitoring agricultural drought in the Lower Mekong Basin using MODIS NDVI and land surface temperature data. *International Journal of Applied Earth Observation and Geoinformation*, 18, 417-427.
- Tian, L., Yuan, S., and Quiring, S.M. (2018). Evaluation of six indices for monitoring agricultural drought in the south-central United States. *Agricultural and Forest Meteorology*, 249, 107-119.
- Unganai, L.S., and Kogan, F.N. (1998). Drought monitoring and corn yield estimation in Southern Africa from AVHRR data. *Remote Sensing of Environment*, 63(3), 219-232.
- Wang, H., Vicente-Serrano, S.M., Tao, F., Zhang, X., Wang, P., Zhang, C., and El Kenawy, A. (2016). Monitoring winter wheat drought threat in Northern China using multiple climate-based drought indices and soil moisture during 2000–2013. *Agricultural and Forest Meteorology*, 228, 1-12.
- Wu, J., Zhou, L., Liu, M., Zhang, J., Leng, S., and Diao, C. (2013). Establishing and assessing the Integrated Surface Drought Index (ISDI) for agricultural drought monitoring in mid-eastern China. *International Journal of Applied Earth Observation and Geoinformation*, 23, 397-410.
- Zargar, A., Sadiq, R., Naser, B., and Khan, F.I. (2011). A review of drought indices. *Environmental Reviews*, 19(NA), 333-349.
- Zhang, J., Mu, Q., and Huang, J. (2016). Assessing the remotely sensed Drought Severity Index for agricultural drought monitoring and impact analysis in North China. *Ecological Indicators*, 63, 296-309.
- Zhang, L., Jiao, W., Zhang, H., Huang, C., and Tong, Q. (2017). Studying drought phenomena in the Continental United States in 2011 and 2012 using various drought indices. *Remote Sensing of Environment*, 190, 96-106.